Available online at www.sciencedirect.com
ScienceDirect
Precambrian Research 149 (2006) 217–230
Precambrian Research
www.elsevier.com/locate/precamres

Sulfur and strontium isotopic compositions of carbonate and evaporite rocks from the late Neoproterozoic–early Cambrian Bilara Group (Nagaur-Ganganagar Basin, India): Constraints on intrabasinal correlation and global sulfur cycle

A. Mazumdar [a,*], H. Strauss [b]

[a] *National Institute of Oceanography, Dona Paula, Goa 403004, India*
[b] *Geologisch-Paläontologisches Institut und Museum, Westfälische Wilhelms, Universität Münster, Correnstrasse 24, D-48149 Münster, Germany*

Received 25 January 2006; received in revised form 4 June 2006; accepted 22 June 2006

Abstract

Sulfur and strontium isotope ratios are presented for carbonate and evaporite rocks from the late Neoproterozoic and early Cambrian Bilara and Hanseran Evaporite Groups, NW India. The sulfur isotopic compositions of trace sulfate in carbonate rocks from the Bilara Group (27.2–42.0‰, average 33.8 ± 3.1‰, $n = 37$) and for calcium sulfate from the Hanseran Evaporite Group (27.5–39.7‰, 32.4 ± 3‰; $n = 25$) are in good agreement with previously determined sulfur isotope values from evaporites and phosphorite deposits of terminal Neoproterozoic to early Cambrian age. Lithological and geochemical results suggest the coeval nature of the Bilara Group and Hanseran Evaporite Group. Fluctuations in the sulfur isotopic composition may at least partially be attributed to intrabasinal bacterial sulfate reduction under sulfate limitation or diagenetic processes. These variations are superimposed on the globally recognized sulfur isotopic enrichment that occurred between 600 and 500 Ma. Similarly, the strontium isotopic composition of Bilara carbonate rocks and Hanseran evaporites are comparable to the contemporaneous global seawater $^{87}Sr/^{86}Sr$ ratios, recording an increase during post-Varangerian time. The rise in Sr isotopic ratio through the late Neoproterozoic and early Cambrian and enrichment of sulfate in ^{34}S may be attributed to high nutrient flux associated with erosion and subsequent burial of sulfide through biogeochemical processes. This process possibly dominated over the fluvial flux of ^{32}S rich sulfate produced by pyrite weathering.

Keywords: Sulfur isotope; Late Neoproterozoic; Cambrian; Evaporite; Carbonate

1. Introduction

Extensive fluctuations in the sulfur isotopic composition of marine sulfate have been recorded across the time window straddling the terminal Neoproterozoic and early Cambrian (Strauss et al., 2001; Schröder et al., 2004). Sulfate bearing rocks of this time are significantly enriched in the heavy sulfur isotope (^{34}S) compared to most of the geological record (e.g., Claypool et al., 1980; Walter et al., 2000; Strauss, 1997, 2004), with examples from anhydrite deposits, phosphorites (Shields et al., 1999, 2004) and limestone/dolomites (Goldberg et al., 2005). These perturbations have been attributed

* Corresponding author. Tel.: +91 8322450493.
E-mail addresses: anmaz2001@yahoo.com (A. Mazumdar), hstrauss@uni.muenster.de (H. Strauss).

0301-9268/$ – see front matter © 2006 Elsevier B.V. All rights reserved.
doi:10.1016/j.precamres.2006.06.008

to changes in the global marine sulfur cycle involving reduced (pyrite, organic bound sulfur) and oxidized (sulfate) reservoirs. Enhanced burial of reduced sulfur, such as pyrite, would shift the marine sulfate sulfur isotopic signal towards enriched values, whereas enhanced pyrite weathering and a concomitant fluvial flux of dissolved sulfate would result in a decrease in $\delta^{34}S$ (Kampschulte and Strauss, 2004). The geochemical changes recorded across the terminal Neoproterozoic and its transition into the early Cambrian have been linked to geological (rearrangement of landmasses: e.g., McKerrow et al., 1992; Meert and Lieberman, 2004) and biological (evolutionary: e.g., Glaessner, 1984; Conway Morris, 1987, 1993) changes. Palaeogeographic reconstructions for this time by Gorin et al. (1982), McKerrow et al. (1992), and Meert and Lieberman (2004) support an equatorial position of the northern part of Gondwanaland. Several fault basins formed due to rifting/wrenching in parts of Gondwanaland stretching from India and Pakistan across the Arabian Shield to the central Iran where great volumes of carbonate (dolomite/limestone) and evaporite deposited (Husseini and Husseini, 1990). Marine-evaporite and carbonate deposits in northwestern India (Nagaur-Ganganagar Basin), Pakistan (Salt Range), Oman (South Oman salt Basin), Iran (Kerman Basin) and Saudi Arabia formed in rift grabens that were in close proximity to each other within a broad carbonate shelf along the western margin of east Gondwanaland (Husseini and Husseini, 1990). Isotopic (stable and radiogenic) studies of chemical sediments, i.e. carbonates and evaporites, provide a unique opportunity for interbasinal correlation. Furthermore, these sediments have archived the compositional state of contemporary marine water allowing the reconstruction of its temporal evolution. Carbonates (Bilara Group) and evaporites (Hanseran Evaporite Group) of the Nagaur-Ganganagar Basin (western India) constitute an important link in a comprehensive correlation of sediments deposited along the northern margin of Gondwana through terminal Neoproterozoic and early Cambrian time. Previous work on the sulfur isotopic composition of sulfate rocks from the Ara Group, Oman Basin (Schröder et al., 2004), the Hormuz Formation, Iran (Houghton, 1980) and the Hanseran Evaporite Group of Nagaur-Ganganagar Basin (Strauss et al., 2001) shows a large spread including highly enriched sulfur isotope values which can be correlated with those recorded from other contemporary marine sulfates (Strauss et al., 2001; Strauss, 2004; Schröder et al., 2004). However, owing to a lack of age control for the sampled sections, to intrabasinal variations and to possible diagenetic factors, the global correlation of sulfur isotopic perturbations, particularly in Precambrian successions, remains a challenging task.

In this paper we report the first set of data on sulfur and strontium isotopic compositions of carbonate rocks from the Bilara Group and strontium isotope values for the correlative Hanseran Evaporite Group of Nagauar-Ganganagar Basin. The latter supplement previously determined sulfate sulfur isotope data (Strauss et al., 2001). In general, the results facilitate intrabasinal and interbasinal correlations. Moreover, an estimate of the broad depositional age is possible based on chemostratigraphic grounds. In addition, possible causes for the marked perturbations in the sulfur (and strontium) isotopic composition of seawater straddling the Precambrian–Cambrian time window are discussed.

2. Geology

2.1. Stratigraphy

The Nagaur-Ganganagar Basin (Fig. 1A), western Rajasthan, India, is an elongated asymmetrical sedimentary basin trending NNE-SSW and covering an area of over 100,000 km^2. It is bounded by the Aravalli Mountain Range in the east, the Delhi–Lahore subsurface ridge in the northeast and north and the Devikot–Nachna subsurface high in the southwest. The Marwar Supergroup (Pareek, 1981) constitutes the late Neoproterozoic–early Cambrian succession in this basin. It rests on Precambrian gneisses, granites and rhyolites belonging to the Malani Group (Fig. 1B). Malani Group rocks reflect polyphase igneous activity, which ranges in age from 780 to 680 Ma (Rathore et al., 1999), providing a basal age limit for the Marwar Supergroup. The Marwar Supergroup consists of: (i) Jodhpur Group, (ii) Bilara Group and (iii) Nagaur Group in ascending order. The Jodhpur Group is a fluvio-marine succession, comprised of cross-bedded, reddish sandstone with maroon shale. The beds dip gently 2–5° towards N and NW. Lenses of conglomerate derived from Malani Rhyolite locally underlie the Jodhpur Group. The Bilara Group comprises dolomite and limestone with occasional clay beds and conformably overlies the Jodhpur Group. The Bilara Group is overlain by a sequence of medium to coarse grained, cross-bedded, reddish brown, sandstone belonging to the Nagaur Group (fluvial). The Hanseran Evaporite Group (HEG, Fig. 1B) is thought to represent a coeval facies variant of the Bilara Group (Dey, 1991) and is underlain and overlain by rocks from the Jodhpur and Nagaur Groups, respectively (Dasgupta et al., 1988; Kumar, 1999). The HEG has been encoun-

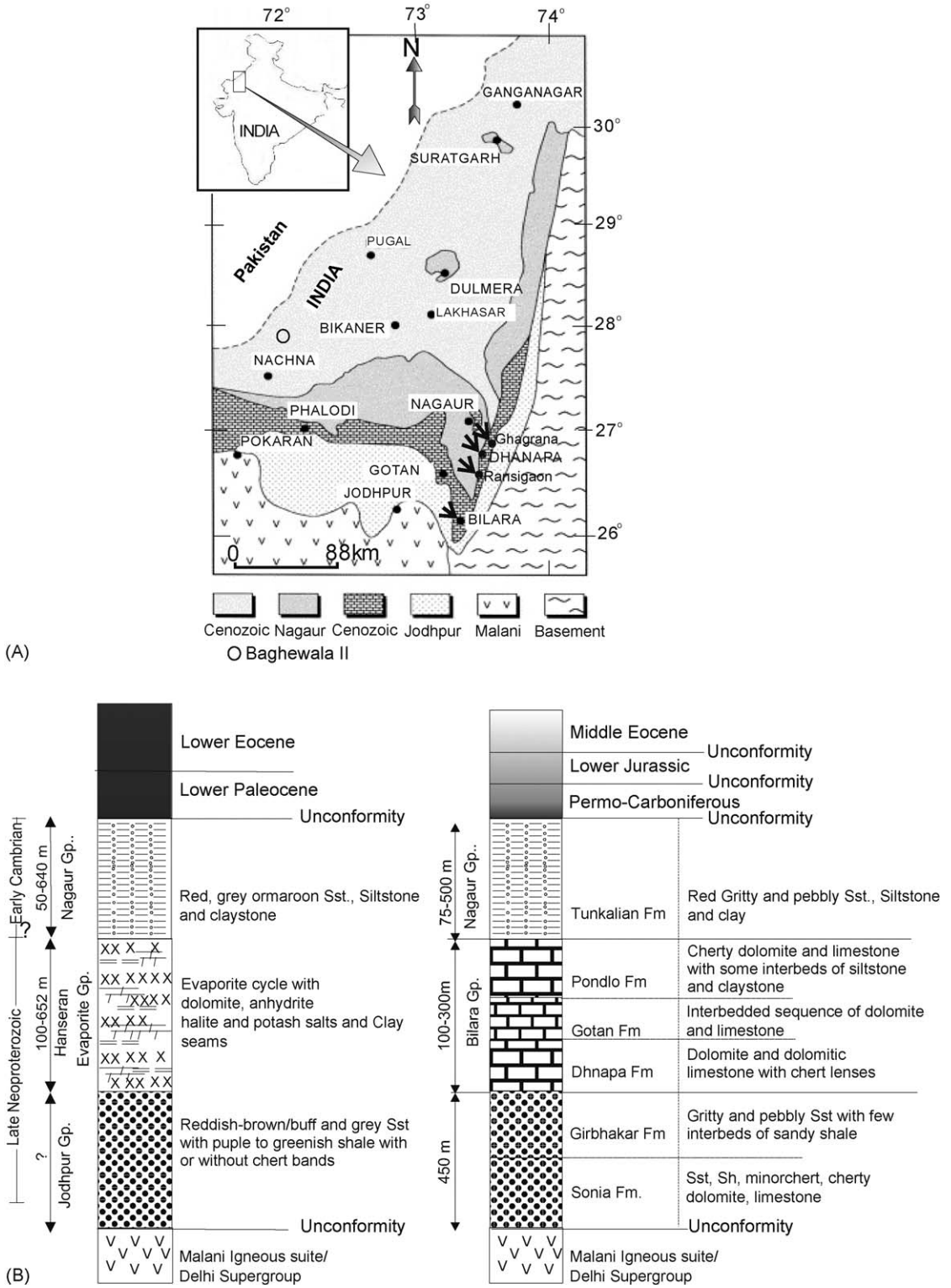

Fig. 1. (A) Map showing the location of the Nagaur-Ganganagar Basin. Sampling locations are marked with arrows. (B) Generalized lithologs of the Marwar Supergroup showing Bilara and Hanseran Evaporite Groups. The Hanseran Evaporite Group is extensively developed in the central and northern parts of the basin and has been mapped through borehole studies (Kumar et al., 1999).

tered in subsurface boreholes and is well developed in the central and northern parts of the Nagaur Basin. A maximum of seven evaporite cycles has been identified from the HEG (Dasgupta, 1996; Kumar, 1999). Each cycle is composed of dolomite, magnesite, anhydrite, halite, polyhalite and clay bands in ascending order. Silvite has also been reported from some bore holes. The presence of organic-rich, finely laminated shale layers and vuggy dolomite (emanating H_2S smell when crushed) suggest intermittent basinal anoxia possibly caused by density stratification during evaporation (Kirkland and Evans, 1981). Rocks of the Marwar Supergroup have also been reported from oil wells (Baghewala I and II) on the western margin of the Nagaur-Ganganagar Basin, with live oil shows in multiple zones (Dasgupta and Balaguda, 1994). Based on geochemical characterization of the crude oil in the Bilara and Jodhpur successions in Baghewala cores, Peters et al. (1995) correlated these oils with the late Neoproterozoic–early Cambrian Huqf oil of southern Oman and Karampur-I oil of East Pakistan and proposed an Infracambrian–Cambrian age for the Bilara carbonates.

2.2. Depositional setup

The carbonate rocks of the Bilara Group are exposed in low-lying hills or quarries along the eastern and southern borders of the Nagaur-Ganganagar Basin. For the present study, samples were collected near Bilara (TG), Dhanapa (DH, HD, HKSPH, K, ANS), Ransigaon (RAN) and Ghagrana (GAG) villages (Fig. 1A). Sedimentary structures observed suggest an arid-peritidal depositional milieu. Horizontal tidal bundles along with current ripple laminations are commonly observed features (Fig. 2A). The horizontal lamination is characterized by alternating fine and coarse carbonate particles. Ripple laminations often show truncations. These current structures typically suggest deposition in an intertidal zone (Reinick and Singh, 1980). Microbial structures (Fig. 2B) are ubiquitous throughout the sections and often display a highly crinkled and contorted nature. The presence of mudcracks (Fig. 2C) suggests subaerial exposure in an arid environment. Well-preserved stromatolitic buildups (Fig. 2D) have been observed at both Dhanapa and Bilara regions. Linked hemispheroidal and conoform types have been recorded. The stromatolitic

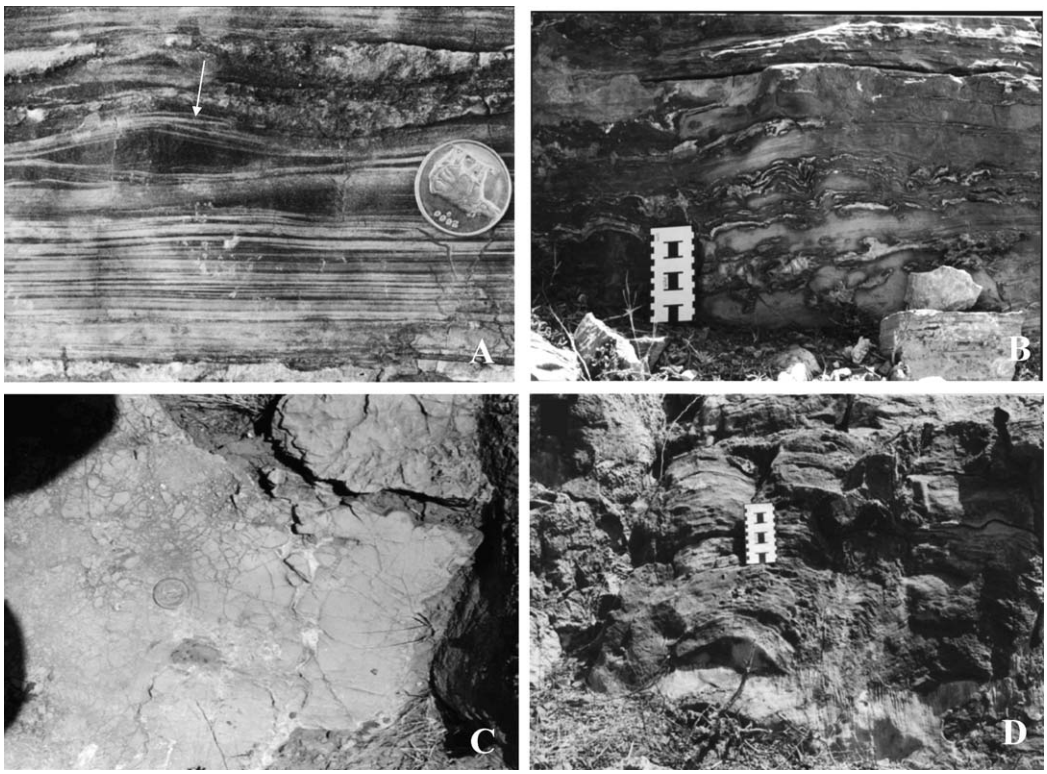

Fig. 2. Sedimentary structures in carbonate rocks of Bilara Group: (A) tidal laminites and truncated ripple structure (arrow); (B) crenulated microbial structures; (C) mudcracks in dolomicrite; (D) domal stromatolites. Diameter of coin = 26 mm, scale length = 15 cm.

buildups constitute a reefal structure in Dhanapa region. The stromatolites here are extensively chertified. Biohermal stromatolites viz., Collenia, Colloniella, Cryptozoon and Irregularia have earlier been reported from the Bilara Group by Barman (1980, 1987).

3. Mineralogy and petrography

Carbonate rocks of the Bilara Group range in composition from pure dolomite to pure calcite and intermediate types with variable percentages of dolomite and calcite (Mazumdar and Bhattacharya, 2006, submitted). Dolomites are characterized by subhedral to euhedral crystals (Fig. 3A) with grain size ranging form ~10 to 20 μm and display both planar and non-planar grain contacts. Compared to dolomites, calcites are characterized coarse crystals (Fig. 3B). Anhydrite crystals although minor in amount have been recorded in many carbonate samples. Anhydrite is present as crystal mush (pseudomorphs after gypsum, Fig. 3C) or as isolated crys-

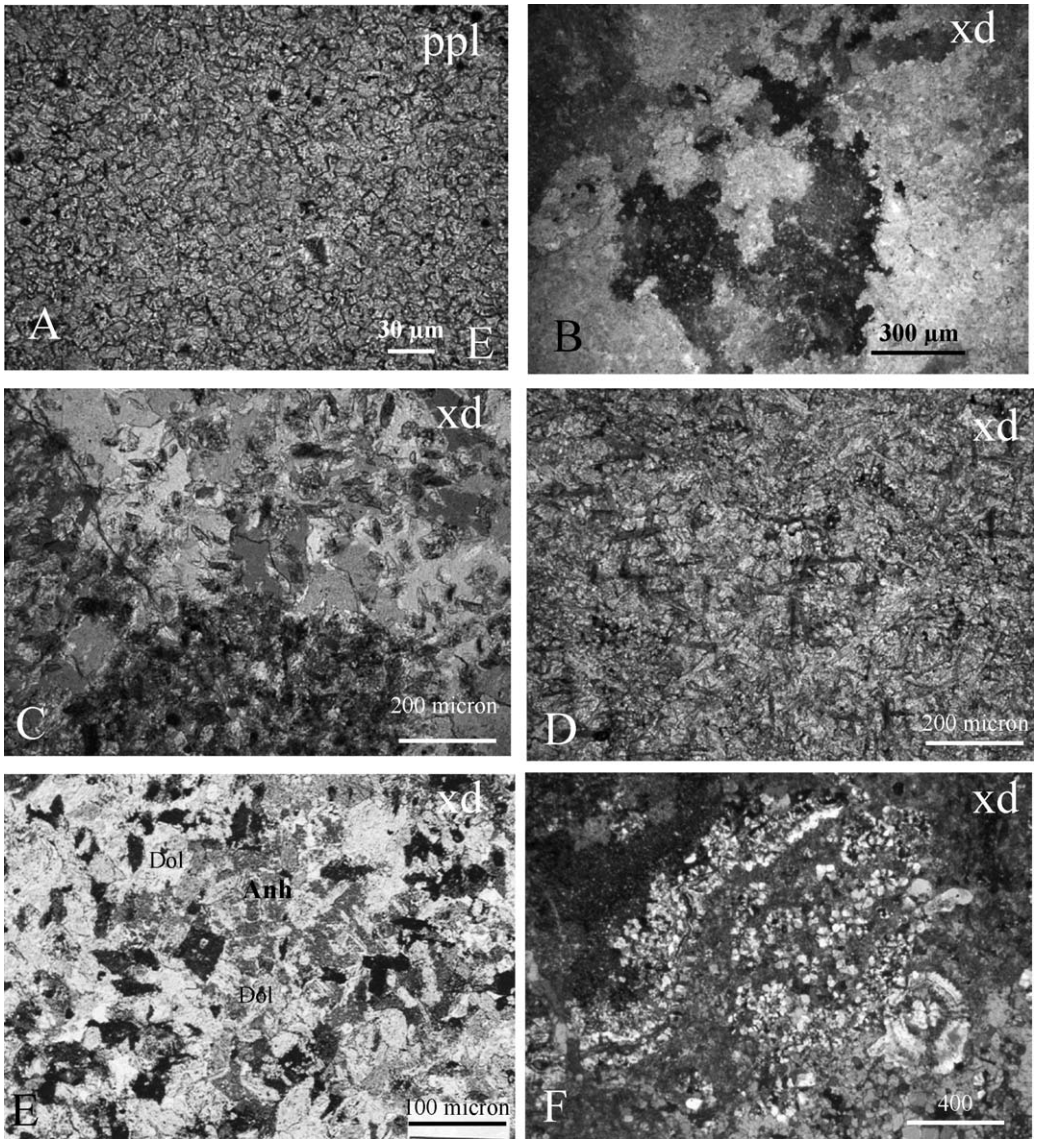

Fig. 3. (A) Fine grained interlocking euhedral to subhedral dolomite crystals. (B) Coarse calcite crystals in limestone. (C) Anhydrite mush in sparry dolomite. Anhydrite crystals show partially corroded grain boundaries and replacement by dolomite. (D) Needle shaped isolated anhydrite crystals within micritic dolomite. Dark colour of the crystals is possibly due to organic enrichment. Anhydrite crystals show peripheral alteration or complete replacement by carbonate. (E) Anhedral, isolated anhydrite crystals within sparry dolomite. (F) Anhydrite nodules replaced by silica. Note the structural zoning within the nodules.

tals within the carbonate matrix (Fig. 3D and E) which are often partially (peripheral alteration) or completely (phantom crystals) replaced by carbonate. Needle shaped anhydrite crystals normally range in size from 60 to 100 μm (occasionally 500–600 μm) and show random orientation. In addition, they sometimes show dark inclusions of organic matter. Silicified anhydrite has also been observed in the Bilara carbonates (Fig. 3F). Anhydrite is replaced by silica as spherules which are in most cases are length slow chalcedony (often riddled with inclusions of anhydrite). The chert spherules commonly show coalesced structure. At least three silica types can be noted in Fig. 3E, outer quartzine, middle drusy quartz and inner radiating mega quartz. Similar textures have been reported by Siedlecka (1972), Milliken (1979), Alonso-Zarza et al. (2002). Owing to a strong matrix effect from calcite and dolomite, anhydrite could not be quantified by X-ray diffractometry.

4. Analytical methods

Fresh pieces of carbonate rocks (30–40 gm) were powdered to 200 mesh size. Sample powders were subjected to 24 h leaching in 0.5 M NaCl solution. This step dissolves the non-structural sulfate (e.g., anhydrite) owing to enhanced solubility in NaCl solution. However, it is difficult to ascertain if minor anhydrite remains undissolved or as trapped grains within carbonate crystals. The filtered residue was later dissolved in 6N HCl with constant stirring at room temperature (25 °C). The solution was filtered through a 0.45 μm cellulose nitrate membrane filter. The insoluble residue amounted to 0.6–7% of the original sample and was mostly composed of quartz, clay (corrensite, montmorillonite and illite), minor organic matter and pyrite. The filtrate was brought to boiling followed by addition of $BaCl_2$ solution. The suspension containing barium sulfate was boiled for half an hour and then kept at around 90 °C overnight for coarsening and purification of the $BaSO_4$ crystals. Low pH of the solution prevents precipitation of any carbonate phase. The $BaSO_4$ precipitate was filtered, dried and weighed.

The sulfur isotopic composition of pyrite from the insoluble residue was measured following wet chemical extraction of sulfur. Chromium reducible sulfur ($S^0 + FeS_2$) was extracted with 1 M $CrCl_2$ solution and 6N HCl in N_2 atmosphere (Canfield et al., 1986). H_2S produced by reduction of sulfide was trapped as ZnS in zinc acetate solution (pH 11) and subsequently reprecipitated as Ag_2S by adding $AgNO_3$ (Canfield et al., 1986). $\delta^{34}S$ of pure $BaSO_4$ and Ag_2S precipitates were combusted with V_2O_5 at 1150 °C in an elemental analyzer. Measurements of the sulfur isotopic composition were performed on a Finnigan MAT Delta plus IRMS with a continuous flow interface and an elemental analyzer (EA or TC/EA) attached to it. All results are reported in standard delta notation ($\delta^{34}S$) as per mil deviations from the VCDT (Vienna Canyon Diablo Troilite). Reproducibility of $\delta^{34}S$ value is better than ±0.3‰ based on repeated measurements of reference materials (NBS-127, IAEA S1, S2) as well as internal laboratory standards. Thirty-seven samples were analyzed for their sulfate sulfur and 16 residues for their sulfide sulfur isotopic composition.

The mineralogical (carbonate and clay) studies were carried out using Siemens D500 and PW3710 X-ray diffractometers. A semi-quantitative estimation of the relative proportions of dolomite and calcite was made following Tennant and Berger (1957). Mn and Sr concentrations of the Bilara carbonate samples were measured by ICP-AES (Seiko SPS 1500) at the University of Nagoya, Japan.

$^{87}Sr/^{86}Sr$ analyses presented in this study were conducted on micro-drilled samples from petrographically selected areas of the apparently best preserved rock matrix. For Sr isotopic analyses ~2–4 mg of carbonate (6 samples) and sulfate powders (10 samples) were dissolved in 2N ultra-pure HCl (Kampschulte et al., 1998). Sr was extracted with HCl on a DOWEX AG-50W8 (200–400 mesh) resin bed in 5 ml columns. Sr was loaded with TaF_5 on W filaments and analyzed on a VG sector 54-30 in dynamic multicollector mode. Repeated analyses of the standard NBS 987 yielded 0.710295 ± 0.000030 ($n = 12$) for $^{87}Sr/^{86}Sr$ ratio.

5. Results

Sulfate concentrations in the Bilara carbonates vary from 0.02 to 0.44% (average $0.08 \pm 0.08\%$) with 50% samples falling within 0.018–0.05% (Table 1). The pyrite content could not be reliably quantified by gravimetry owing to very low concentrations. Sulfate concentrations in the Bilara carbonates are higher than those reported from normal Neoproterozoic carbonates (Hurtgen et al., 2002; Goldberg et al., 2005). Staudt and Scoonen (1995) reported structural sulfate (in carbonate rock) concentrations ranging from 0.06 to 0.7% in evaporitic dolomite. High sulfate concentrations in carbonates of Bilara Group could well be attributed to its arid and evaporitic depositional setup. Presence of some residual anhydrite may also result in high sulfate concentrations as recorded for some samples. However, mixture of two different sulfate sources viz., anhydrite and sulfate in carbonate mineral lattice is not expected to cause any major difference is S isotopic composition. This is corrobo-

Table 1
Mineralogy and sulfur isotopic compositions of sulfate and chromium reducible sulfide (CRS) in Bilara carbonates

Sample number	Mineralogy	Strctural SO_4 (%)	δ^{34}S-sulfate (‰) (CDT)	δ^{34}S-CRS (‰) (CDT)
TG/6/3/5	60% calcite	0.07	30.6	nd
TG/7/3/7	Calcite	0.44	31.8	21.65
TG 8-7	Calcite	0.06	31.3	nd
TG 8-10	Calcite	0.04	31.1	19.89
TG 9	60% calcite	0.02	30.0	nd
TG 10	Calcite	0.04	34.2	3.21
TG 11	Dolomite	0.04	31.7	nd
TG 15	Dolomite	0.04	33.5	nd
TG 16	Dolomite	0.03	27.3	nd
TG 17	Dolomite	0.04	31.0	−2.75
TG 22(2)	Dolomite	0.02	28.7	nd
TG 29	Calcite	0.03	31.4	nd
TG 32	Calcite	0.03	31.5	−2.54
TG 36	Calcite	0.10	31.0	nd
TG 37	Calcite	0.16	31.6	12.41
TG 39	Calcite	0.06	32.9	11.3
TG 43	Calcite	0.04	31.1	nd
K 1	nm	0.08	36.4	12.14
K 2	Calcite	0.26	36.3	nd
K 5	Calcite	0.07	35.0	nd
K 8	Calcite	0.08	36.1	nd
K 10	Calcite	0.20	35.7	17.49
K 11	Dolomite	nm	35.7	nd
K 13	Dolomite	0.07	34.4	10.56
K 14	Dolomite	0.09	35.9	nd
DH/11/3/1	Dolomite	0.10	36.5	8.34
DH/11/3/25	Dolomite	0.11	36.3	14.2
GAG-8	Calcite	0.03	34.5	nd
GAG 10	Dolomite	0.10	33.4	nd
GAG 15	Dolomite	0.04	34.4	8.26
ANS-1	Calcite	0.06	36.2	nd
RAN 7	Dolomite	0.03	41.8	10.99
RAN-1	nm	0.03	42.0	nd
HKSPH 3	nm	0.04	36.0	nd
HKSPH-4	nm	0.04	35.7	7.45
HD/9/3	nm	0.05	33.0	nd
HD 9/3/4	nm	0.09	34.4	11.2
K-5 NaCl	NaCl filtrate		34.3	

CDT = Canyon Diablo Troilite, nm = not measured.

rated by the fact that sample K-5 NaCl (NaCl filtrate: $\delta^{34}S = 34.3‰$) is similar to K-5 (NaCl leached residue: $\delta^{34}S = 35‰$; Table 1). However, it is not expected in rocks with high pyrite content owing to artifact sulfate production by pyrite weathering. In case of Bilara carbonate, pyrite content is negligible.

The sulfur isotopic compositions for sulfate in the Bilara Group carbonates are given in Table 1 and graphically represented in Fig. 4. $\delta^{34}S_{SO_4}$ ranges from 27.2 to 42.0‰ (average $33.8 \pm 3.1‰$, $n = 37$). The sulfur isotopic composition of pyrite ranges from −2.5 to +21.6‰.

$^{87}Sr/^{86}Sr$ ratios for the carbonate rocks of Bilara Group (Table 2A) vary from 0.70817 to 0.70848 (0.70832 ± 0.000354, $n = 5$) excluding one sample ANS-4 which shows a high value of 0.70915. It is apparent from the data that the highest Sr isotope ratio corresponds to the lowest Sr concentration. We have not considered Sr isotope ratio of ANS-4 in our interpretation owing to the possible diagenetic alteration. Low Mn concentration, low Mn/Sr ratios (0.06–0.33) and oxygen isotope ratios (−3.1‰ to 4.7‰) suggest minimum meteoric water alteration (Kaufman and Knoll, 1995) for the Bilara samples measured for Sr isotope ratio. $^{87}Sr/^{86}Sr$ ratio for anhydrite from the HEG varies from 0.70812 to 0.708965 (average = 0.70856 ± 0.00026, $n = 10$) (Table 2B). In the absence of geochemical tests for possible alteration of the Sr isotope ratio of anhydrites, we have tentatively assumed that the

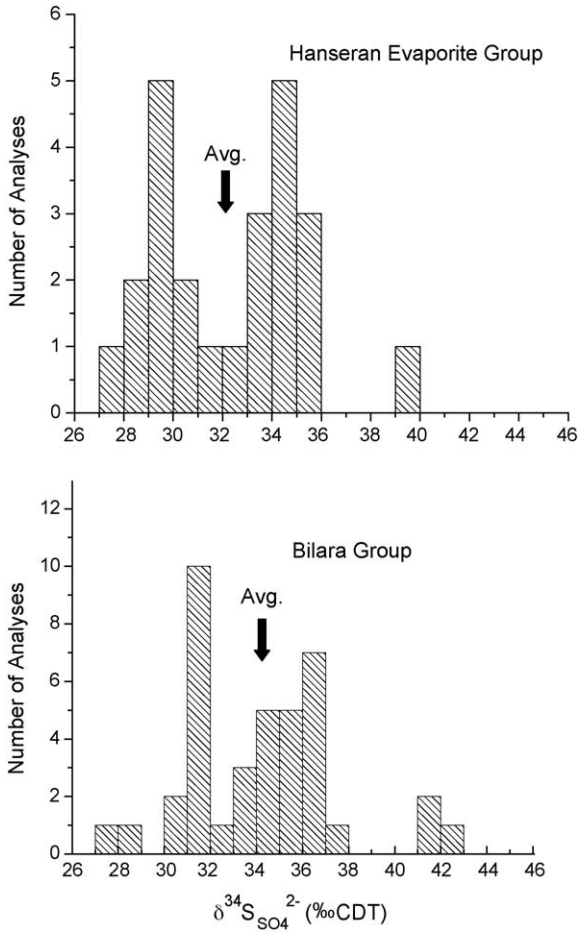

Fig. 4. Histograms showing sulfur isotopic composition of sulfate in Bilara and Hanseran Evaporite Groups. Average compositions are marked with arrows.

Sr isotope ratios close to the well-preserved Bilara carbonates as diagenetically least altered. Petrographic studies of anhydrite and carbonates from cores P-47 and P-12 and P-4 of Hanseran evaporites (Grover, 1997; Mishra, 1998) show predominantly micritic anhydrite. Anhydrites of P-47 and P-12 and P-4 were studied by Strauss et al. (2001) for sulfur isotopic composition referred in the present paper. Sr isotopic compositions presented here are from the same sample sets.

6. Discussion

6.1. Intrabasinal correlation

Owing to the lack of a proper basin evolution model and radiogenic dates, intrabasinal correlation of the Bilara and Hanseran Evaporite Groups had so far been quite conjectural. However, newly determined strontium and sulfur isotopic ratios from this study lend support to the contention that rocks of the Bilara Group and the HEG are coeval facies variants. $^{87}Sr/^{86}Sr$ ratios (Table 2A and B) and $\delta^{34}S_{SO_4}$ (Fig. 4) values are close for the two groups. Based on a correlation of carbon isotopic studies, Mazumdar and Bhattacharya (2004) and Pandit et al. (2001) expressed similar views.

Strauss et al. (2001) recorded $\delta^{34}S_{SO_4}$ through a composite HEG succession which ranges from 29.7‰ to 35.6‰ and a subsequent decline to 29.6‰. Such variation is also reflected in the carbonate rocks of the Bilara Group with two maxima at around 3l‰ and 36‰. Based on sedimentological and geochemical data, it is possible to reconstruct the basinal evolution of Nagaur-Ganganagar Basin during terminal Neoproterozoic and early Cambrian times (Fig. 5). The Nagaur-Ganganagar Basin remained tectonically unstable as indicated by the presence of several steeply dipping faults (Kumar, 1999). Tectonic subsidence of the basin controlled the accumulation of a 652 m thick evaporite succession. Based on borehole data, Kumar (1999) suggested an asymmetric depositional pattern for the carbonate, sulfate and halite. Closed basinal conditions were established after the deposition of the Jodhpur sandstone. The presence of several evaporite cycles (up to seven) in the HEG suggests repeated episodes of marine water influx into a closed basin followed by evaporative concentration of salts under arid conditions. It is apparent that the Bilara carbonates were deposited on the edges of the basin whereas sulfate and halite were deposited in an asymmetric pattern in the central and northern parts. By contrast to the HEG, no evaporite beds have been reported within the Bilara Group carbonate succession. It may be concluded that the carbonate rocks of the Bilara Group essentially represent marginal carbonate sediments of the Hanseran evaporite basin.

6.2. Intrabasinal sulfur isotopic variations

The observed sulfur isotopic composition measured in sulfate from carbonate rocks of the Bilara Group and from evaporitic sulfate of the Hanseran Evaporite Group are in good agreement with previously determined isotope values from evaporites and phosphorite deposits of late Ediacaran–early Cambrian age (Strauss, 1997, 2004; Strauss et al., 2001; Shields et al., 1999, 2004). Still, it is important to assess whether the observed isotope signatures were overprinted by fluctuations in the basinal sulfur geochemistry. This is also pertinent when considering the significant spread in the sulfur isotopic composition of seawater sulfate over this time window (Fig. 6). The presence of foetid dolomite and dark organic-rich car-

Table 2
Strontium isotopic composition of carbonates and anhydrites of Bilara and Hanseran evaporite Groups, respectively

Sample number	Mineralogy	Delta18O	Mn/Sr	Mn (ppm)	Sr (ppm)	$^{87}Sr/^{86}Sr$	IR (%)
A							
ANS-1	Cal	−1.97	0.11	16.7	147	0.70835	2.10
K 8	Cal	−3.1	0.22	36.4	164.9	0.70825	0.80
K 9	Dol + cal	3.75	0.25	37.8	151	0.70837	1.83
K 10	Cal	1.65	0.06	21.7	320.3	0.70817	3.70
ANS-4	Dol + cal	1.5	0.33	38.8	116	0.70915	0.80
DH11/3/17	Dol + cal	4.66	nm	nm	nm	0.70848	nm

Sample number	Mineralogy	$^{87}Sr/^{86}Sr$
B		
550.1	Anhydrite	0.708706
558	Anhydrite	0.708592
562.8	Anhydrite	0.708553
573.35	Anhydrite	0.708442
590	Anhydrite	0.708778
599.5	Anhydrite	0.70816
613.75	Anhydrite	0.708965
641	Anhydrite	0.708722
273.8	Anhydrite	0.70859
704	Anhydrite	0.708122

nm = not measured.

bonate as well as shale layers in both, the Bilara Group and the Hanseran Evaporite Group, suggest intermittent anoxia due to salinity stratification in a closed basin following fresh influx of seawater. High algal biomass and sulfate should promote extensive bacterial sulfate reduction (BSR). Bacterially mediated dissimilatory sulfate reduction involves reduction of dissolved SO_4 to H_2S via a series of complex enzymatically catalyzed biochemical reactions coupled with organic matter oxidation (Canfield, 2001; Goldhaber, 2003; Megonigal et al., 2003 and references therein). Thereby, hydrogen sulfide is enriched in ^{32}S relative to ^{34}S (Harrison and Thode, 1958; Dettmers et al., 2001). H_2S reacts with easily reducible ferric compounds (e.g., FeOOH) forming pyrite (Berner, 1984). However, under iron limited conditions, H_2S may either be lost from the system or trapped by organic molecules as organo-sulfur compounds. Very low pyrite contents in rocks of the Bilara and Hanseran Evaporite groups suggest iron limited conditions. In addition, under sulfate limited conditions, bacterial sulfate reduction (BSR) would lead to enrichment in ^{34}S in the residual sulfate following Rayleigh fractionation. Schröder et al. (2004) reported a mean value of 39.4‰ (32–46‰) for $\delta^{34}S_{SO_4}$ from the Ara Group (Oman) evaporites and attributed it to BSR under sulfate limited conditions. Sediments of both, the Bilara Group and the Hanseran Evaporite Group show $\delta^{34}S_{SO_4}$ values of up to 42‰, suggesting a similar situation.

Keeping in view the shallow marine conditions that prevailed in the Nagaur-Ganganagar Basin during the development of the evaporite sedimentary package, oxidation of H_2S at the oxic–anoxic interface cannot be ruled out. Subsequently, this may also lead to disproportionation of elemental sulfur (S^0) or sulfur-bearing intermediates such as thiosulfate ($S_2O_3^{2-}$) and sulfite (SO_3^{2-}). It is well documented that disproportionation is associated with a large sulfur isotope fractionation between residual sulfate and sulfide by depleting the sulfide in ^{34}S through repeated steps of sulfide oxidation and disproportionation (Canfield and Thamdrup, 1994; Habicht et al., 1998; Böttcher et al., 2001). Absence of highly ^{34}S depleted pyrite in Bilara carbonates is possibly due to overprinting by late diagenetic pyritisation in the sediment from ^{34}S-enriched residual fluids during burial.

6.3. Late Neoproterozoic sulfur isotopic enrichment

As a consequence of a large residence time for sulfate (20×10^6 years) compared to the ocean mixing time (~1500 years), contemporary marine sulfate precipitates (mainly calcium and barium sulfate) record the same isotopic composition. Hence, the sulfur isotopic composition of marine sulfate is considered an important geochemical proxy for evaluating the global marine geochemical evolution and a further option for interbasinal

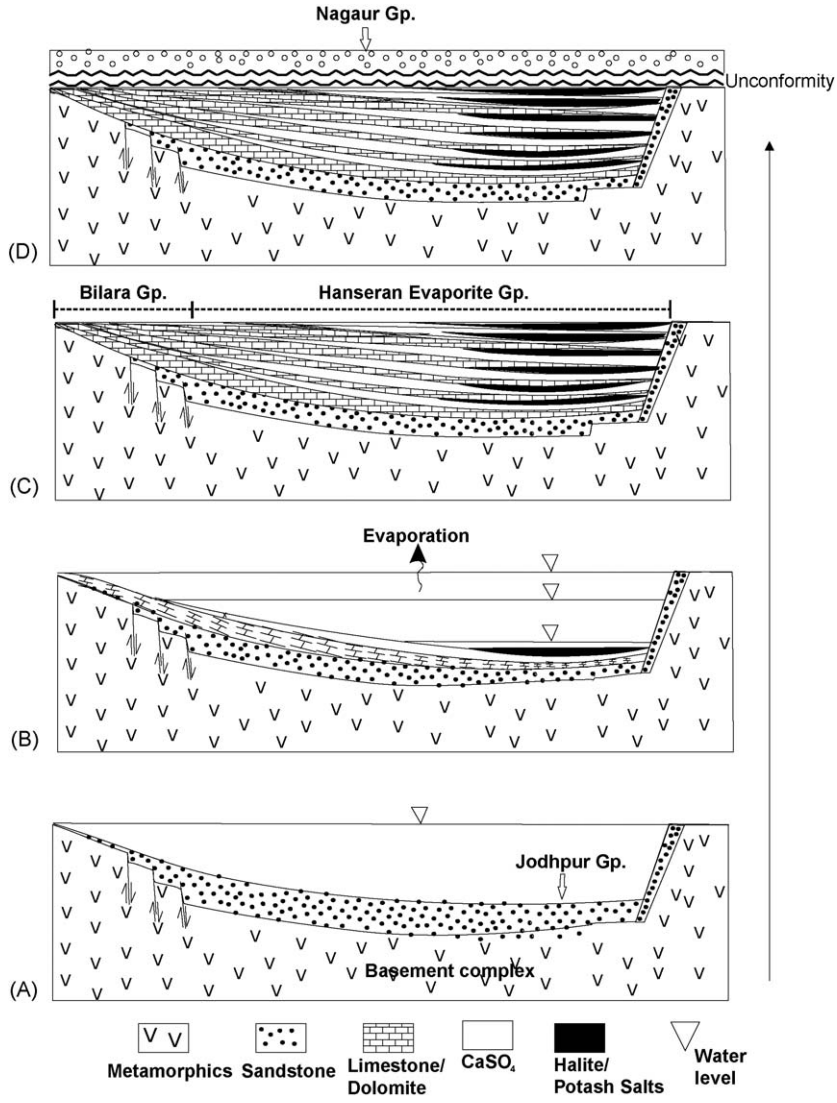

Fig. 5. A schematic basin evolution model for the Marwar Supergroup depicting temporal and spatial relationship between the Bilara and Hanseran Evaporite Groups.

correlation. Despite possible basinal effects, the heavy $\delta^{34}S$ values recorded for sulfate sulfur from the Bilara Group and the Hanseran Evaporite Group are consistent with the general trend of the global sulfate sulfur isotope curve through the terminal Neoproterozoic and Cambrian time interval (Fig. 6). The rise in the sulfur isotope ratio towards the late Neoproterozoic (average 32‰, Strauss, 2004) relative to the early Neoproterozoic (average 18‰) reflects a major change in sulfur isotope mass balance in the contemporary global ocean. The sulfur isotopic composition of seawater sulfate is a function of pyrite deposition and preservation in marine sediments and pyrite weathering and subsequent fluvial transport as dissolved sulfate into the ocean. The former process is a result of bacterial sulfate reduction favoring the incorporation of the light ^{32}S isotope into the pyrite and, hence, leads to an increase in the ^{34}S of dissolved sulfate and contemporary sulfate mineral precipitates. On the other hand pyrite weathering is expected to contribute ^{32}S-enriched sulfate to the dissolved sulfate pool.

Alternatively, a rise in ^{34}S of oceanic sulfate has been proposed in connection with phases of enhanced continental weathering (e.g., Kampschulte et al., 2001; Kampschulte and Strauss, 2004). The latter process delivers substantial amounts of nutrients to the ocean, triggering an increase in primary productivity. Subsequent delivery of organic matter to the sediment in turn results in increasing rates of bacterial sulfate reduction,

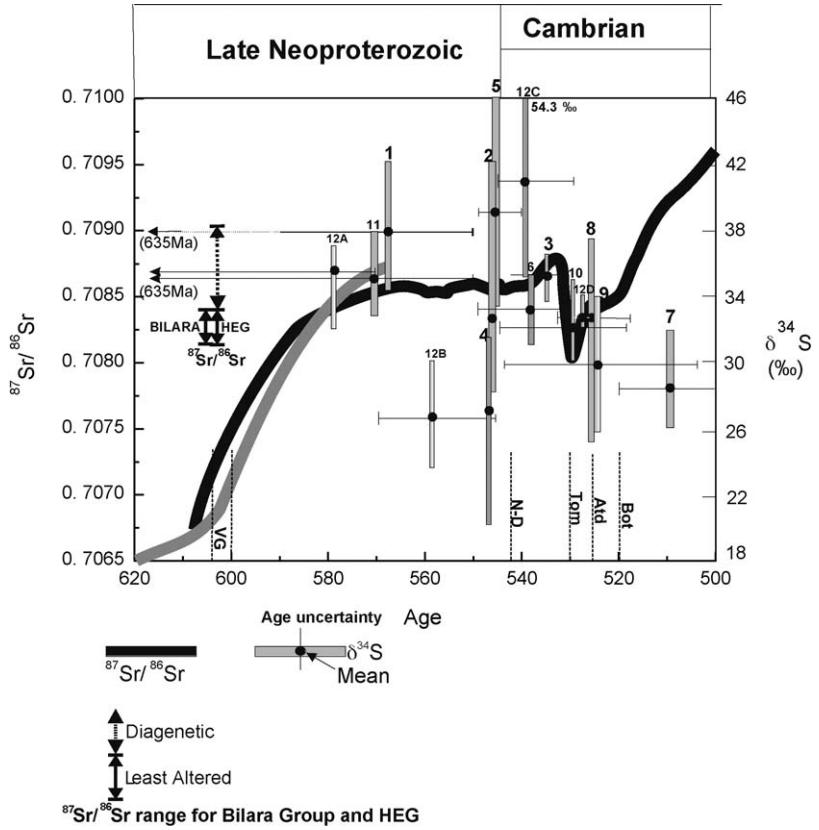

Fig. 6. Temporal variations of sulfur and strontium isotopic compositions of seawaters through late Proterozoic and Cambrian. Sulfur isotopic compositions recorded for terminal Proterozoic and Cambrian from different basins are plotted for comparison. (1) Doushantuo Fm. (China, Shen et al., 2000), (2) Bilara and Hanseran Evaporite Groups (this study and Strauss et al., 2001), (3) Danilovo (Siberia, Vinogradov et al., 1994; cf. Peryt et al., 2005), (4) Hormuz Formation (Iran, Houghton, 1980), (5) Ara Group (Oman, Schröder et al., 2004), (6) Zhongyicun (China, Shields et al., 1999), (7) Amadeus Basin, Australia (Claypool et al., 1980; Walter et al., 2000), (8) Yuhucun Fm. (China, Shields et al., 1999; Shen et al., 2000), (9) Angarskya (Siberia, Claypool et al., 1980), (10) Motskya (Claypool et al., 1980), (11) Doushantuo Formation (Shields et al., 2004), and (12A–D) Doushantuo, Dengying, Nemakit-Daldynian and Tommotian of Yangtze Platform, China (Goldberg et al., 2006). Upper age limit for Doushantuo Formation from Condon et al. (2005). The range for strontium isotopic ratios for the presumably least altered carbonates and evaporites of Bilara Group and Hanseran Evaporite Groups (HEG) are plotted as double sided solid arrows. Sr isotopic ratios of HEG anhydrites showing possible diagenetic alteration is represented by double sided dotted arrow. VG, Varanger glaciation; N-D, Nemakit-Daldynian; Tom, Tommotian; Atd, Atdbannian; Bot, Botomian.

extracting a higher proportion of the lighter isotope ^{32}S and leaving behind a ^{34}S-enriched residual global sulfate pool (e.g., Strauss, 2004). The sulfur isotopic composition of the contemporary dissolved sulfate would depend on the relative significance fluvial input of sulfate from terrestrial pyrite weathering and marine sulfide burial. On the other hand, Shields et al. (1999) invoked the hypotheses of increase in isotopic discrimination between sulfide and sulfate by bacterially mediated disproportionation reaction (Canfield and Teske, 1996).

Two contrasting hypotheses have been proposed to explain the rise in the sulfate sulfur isotopic composition (by pyrite burial and sulfate limitation) through the Ediacaran to early Cambrian: a salinity driven oceanic stratification with deepwater anoxia (Holser, 1977) or the development of an ice-covered global ocean in connection with the Snowball Earth hypothesis (Hoffman et al., 1998), both followed by subsequent upwelling of water masses enriched in $\delta^{34}S_{SO_4}$ onto the shelf regions.

Identification of an enhanced input of dissolved material into the ocean, resulting from continental weathering, has been assessed through the $^{87}Sr/^{86}Sr$ ratio of marine chemical sediments (limestone, dolomite, barium sulfate and calcium sulfate). Continental weathering represents one of two principal sources which govern the isotopic ratio of strontium in the ocean (Bickle et al., 2001, 2003). Temporal variations in $^{87}Sr/^{86}Sr$ ratio record changes in the balance between Sr fluxes to the ocean from hydrothermal fluid–rock interaction at mid-ocean ridges and from continental weathering

(Palmer and Edmond, 1989). The $^{87}Sr/^{86}Sr$ composition of the seafloor hydrothermal flux is buffered at low values of ~0.703–0.705. On the other hand continental weathering contributes Sr with a high $^{87}Sr/^{86}Sr$ value (0.709–0.730) via riverine flux to the ocean. Unaltered marine carbonates and evaporites faithfully record ambient seawater $^{87}Sr/^{86}Sr$, given the negligible fractionation of Sr isotopes and the homogenous distribution of Sr isotopes in seawater (DePaolo and Ingram, 1985; Veizer et al., 1999).

Compilation of Sr isotopic composition (Fig. 6) for late Neoproterozoic and Cambrian (Asmerom et al., 1991; Brasier et al., 2000; Derry et al., 1994; Jacobsen and Kaufman, 1999; Kaufman et al., 1993; Melezhik et al., 2001; Misi and Veizer, 1998; Montanez et al., 2000; Nicholas, 1996) is characterized by a rapid rise in $^{87}Sr/^{86}Sr$ ratios from a low of ~0.7065–0.7070 at around 610 Ma to a high of 0.7085 at 580 Ma and form a plateau up to the base of Nemakit-Daldynian. Jacobsen and Kaufman (1999) reported a further rise to 0.7087 in Nemakit-Daldynian and subsequent rapid fall to a low of 0.7080 in Tommotian followed by a steady rise to 0.7095 up to late Cambrian (Derry et al., 1994; Nicholas, 1996). The rise in $^{87}Sr/^{86}Sr$ through the terminal Neoproterozoic and early Cambrian has been linked to orogenic activities related to the break-up of Rodinia and subsequent assembly of Gondwana (Pan-African-Brasiliano orogeny: Asmerom et al., 1991; Burns et al., 1994; Derry et al., 1994; Montanez et al., 2000) which resulted in a major phase of continental weathering and riverine flux of highly radiogenic Sr. $^{87}Sr/^{86}Sr$ ratios of possibly least altered carbonates of Bilara Group (0.70817–0.708418) and evaporites of HEG (0.70812–0.708442) are consistent with a terminal Neproterozoic to early Cambrian age.

Looking at the sulfate sulfur isotopic composition, $\delta^{34}S_{SO_4}$ shows a significant rise following the level of the Varangerian glaciation and remains high until the late Cambrian (e.g., Shields et al., 1999, 2004; Strauss, 2004). This increase in $\delta^{34}S$ observed during this study would be consistent with a scenario in which post-glacial upwelling of ^{34}S-enriched deepwater onto the shelf and subsequent precipitation of chemical sediments accompanied by the incorporation of this distinct isotopic signature. It would also be consistent with a scenario in which the enhanced delivery of nutrients from continental weathering resulted in increasing primary production and greater subsequent remineralization of sedimentary organic matter, causing sulfate limitation and a Rayleigh-type isotopic fractionation. The biogeochemical process responsible for burial of lighter sulfur was apparently more significant than its contribution via pyrite weather and fluvial flux in to ocean. Hence the rises in Sr and S isotopic compositions through late Neoproterzoic–early Cambrian and possible erosional and nutrient flux into contemporary oceans are apparently linked processes as observed in Phanerozoic with $\delta^{34}S$ and $^{87}Sr/^{86}Sr$ correlation (Veizer et al., 1999).

7. Conclusions

Carbonate and evaporite rocks of the Bilara Group and the Hanseran Evaporite Group, Marwar Supergroup, are coeval facies variants. Sedimentological studies suggest an arid carbonate tidal flat type depositional environment for the Bilara Group rocks. These Bilara carbonates form the marginal carbonate facies of the Nagaur-Ganganagar Basin. Simultaneously, thick deposits of anhydrite and halite formed in the central and northern part of the basin. Sulfur and strontium isotope ratios for sedimentary rocks from both groups are quite similar and justify the interpretation that sediments from both groups were deposited within the same age brackets.

The sulfur isotopic composition for samples from both groups is in good agreement with the globally observed trend of ^{34}S-enriched marine sulfate sulfur during Ediacaran and much of Cambrian time. Intrabasinal variations in the sulfur isotopic composition of dissolved sulfate via bacterial sulfate reduction and/or via disproportionation of sulfur intermediates might have caused additional fluctuations in the sulfur isotopic composition of dissolved sulfate and subsequent chemical precipitates. Such an effect would be superimposed on the global sulfur isotopic signature, making global correlations more challenging. Apparent rise in Sr isotopic ratio through the late Neoproterozoic and early Cambrian and enrichment of sulfate in ^{34}S may tentatively be attributed to high nutrient flux associated with erosion and subsequent burial of sulfide through biogeochemical processes. This process presumably dominated over the fluvial flux of ^{32}S rich sulfate produced by pyrite weathering.

Acknowledgements

Funding for this research by the Deutsche Forschungsgemeinschaft is gratefully acknowledged. The Alexander-von-Humboldt Foundation supported the stay of Aninda Mazumdar. This is NIO contribution 4167.

References

Asmerom, Y.A., Jacobsen, S.B., Butterfield, N.J., Knoll, A.H., 1991. Sr isotope variations in Late Proterozoic seawater: implications for crustal evolution. Geochim. Cosmochim. Acta 55, 2883–2894.

Alonso-Zarza, A.M., Sanchez-Moya, Y., Bustillo, M.A., Sopena, Delgado, A., 2002. Silicification and dolomitization of anhydrite nodules in argillaceous terrestrial deposits: an example of meteoric-dominated diagenesis from the Triassic of central Spain. Sedimentology 49, 303–317.

Barman, G., 1980. An analysis of Marwar Basin, western Rajasthan in the light of stromatolite, chronostratigraphy and utility. Geol. Surv. India Misc. Pul. 44, 292–297.

Barman, G., 1987. Stratigraphic Position of Marwar Supergroup in the Light of Stromatolites. Special Publication, vol. 11. Geological Survey of India, pp. 72–80.

Berner, R.A., 1984. Sedimentary pyrite formation: an update. Geochim. Cosmochim. Acta 48, 605–615.

Bickle, M.J., Harris, N.B.W., Bunbury, J.M., Chapman, H.J., Fairchild, I.J., Ahmad, T., 2001. Controls on the $^{87}Sr/^{86}Sr$ ratios of carbonates in the Garhwal Himalaya, Headwaters of the Ganges. J. Geol. 109, 737–753.

Bickle, M.J., Bunbury, J., Chapman, H.J., Harris, N.B.W., Fairchild, I., Ahmad, T, 2003. Fluxes of Sr into the headwater of the Ganges. Geochim. Cosmochim. Acta 67, 2567–2584.

Böttcher, M.E., Thamdrup, B., Vennemann, T., 2001. Oxygen and sulphur isotope fractionation during anaerobic bacterial disproportionation of elemental sulphur. Geochim. Cosmochim. Acta 65, 1601–1609.

Brasier, M., McCarron, G., Tucker, R., Leather, J., Aleen, P., Shields, G., 2000. New U–Pb zircon dates for the Neoproterozoic Ghubrah glaciation and for the top of the Huqf Supergroup. Oman. Geol. 28, 175–178.

Burns, S.J., Haudenschild, U., Matter, A., 1994. The strontium isotopic composition of carbonates from the late Preacambrian (*c*.560-540) Huqf Group of Oman. Chem. Geol. 111, 269–282.

Canfield, D.E., 2001. Biogeochemistry of sulfur isotopes. Rev. Miner. Geochem. 43, 607–636.

Canfield, D.E., Raiswell, R., Westrich, J., Reaves, C., Berner, R.A., 1986. The use of chromium reduction in the analysis of inorganic sulphur in sediments and shales. Chem. Geol. 54, 149–155.

Canfield, D.E., Teske, A., 1996. Isotope fractionation by sulfate-reducing natural populations and the isotopic composition of sulfide in marine sediments. Nature 382, 127–132.

Canfield, D.E., Thamdrup, B., 1994. The production of 34S-depleted sulfide during bacterial disproportionation of elemental sulfur. Science 266, 1973–1975.

Claypool, G.E., Holser, W.T., Kaplan, I.R., Sakai, H., Zak, I., 1980. Age curves of sulfur and oxygen isotopes in marine sulfate and their mutual interpretation. Chem. Geol. 28, 199–206.

Condon, D., Zhu, M., Bowring, S., Wang, W., Yang, A., Jin, Y., 2005. U–Pb ages from the Neoproterozoic Doushantuo formation. Chin. Sci. 308, 95–98.

Conway Morris, S., 1987. The search for the Precambrian–Cambrian boundary. Am. Sci. 75, 156–167.

Conway Morris, S., 1993. Ediacaran like fossils in Cambrian Burgess Shale-type faunas of North America. Palaeont 36, 593–635.

Dasgupta, U., 1996. Marwar Supergroup evaporites, Rajasthan. In: Bhattacharya, A. (Ed.), Recent Advances in Vindhyan Geology, vol. 36. Gological Society of India, pp. 49–58.

Dasgupta, U., Balaguda, S.S., 1994. An overview of geology and hydrocarbon occurrences in the western part of Bikaner-Nagaur Basin. Indian J. Petrol. Geol. 3, 1–17.

Dasgupta, S.P., Ramachandra, K.V., Jairam, M.S., 1988. A framework analysis of Nagaur Ganganagar evaporite Basin, Rajasthan. Indian Miner. 42, 57–64.

DePaolo, D.J., Ingram, B.L., 1985. High resolution stratigraphy with strontium isotopes. Science 227, 938–941.

Deny, L.A., Brasier, M.D., Corfield, R.M., Rozanov, A.Yu., Zhuravlev, A.Yu., 1994. Sr and C isotopes in lower Cambrian carbonates from the Siberian craton: a paleoenvironmental record during the 'Cambrian explosion'. Earth Planet. Sci. Lett. 128, 671–681.

Dettmers, J., Brüchert, V., Habicht, K.S., Kuever, J., 2001. Diversity of sulfur isotope fractionations by sulphate-reducing prokaryotes. Appl. Environ. Microbiol. 67, 888–894.

Dey, R.C., 1991. Trans-Aravalli vindhyan evaporites under the semidesertic plains of western India: significance of depositional features. J. Geol. Soc. India 37, 136–150.

Glaessner, M.F., 1984. The Dawn of Animal Life: A Biohistorical Study. Cambridge University Press, 244 pp.

Goldberg, T., Poulton, S.W., Strauss, H., 2005. Sulphur and oxygen isotope signatures of late Neoproterozoic to early Cambrian sulphate, Yangtze Platform, China: diagenetic constraints and seawater evolution. Precamb. Res. 137, 223–241.

Goldhaber, M.B., 2003. Sulfur-rich sediments. In: Mackenzie, F.T. (Ed.), Treatise on Geochemistry, vol. 7. Elsevier, pp. 257–288.

Gorin, G.E., Racz, L.G., Walter, M.R., 1982. Late Precambrian–Cambrian sediments of Huqf Group, Sultanate of Oman. AAPG Bull. 66, 2628–2648.

Grover, S., 1997. Evaporite sequence along the borehole no. p/47, Lakhasar, Bikaner district, Rajasthan, India. Unpublished M.Sc. Dissertation. University of Delhi, 46 pp.

Habicht, K.S., Canfield, D.E., Rethmeier, J., 1998. Sulfur isotope fractionation during bacterial reduction and disproportionation of thiosulfate and sulfite. Geochim. Cosmochim. Acta 62, 2585–2595.

Harrison, A.G., Thode, H.G., 1958. Mechanism of the bacterial reduction of sulphate from isotopic fractionation studies. Faraday Soc. Trans. 54, 84–92.

Hoffman, P.F., Kaufman, A.J., Halverson, G.P., Schrag, D.P., 1998. A Neoproterozoic snowball earth. Science 281, 1342–1346.

Holser, W.T., 1977. Catastrophic chemical events in the history of the ocean. Nature 267, 403–408.

Houghton, M.L., 1980. Geochemistry of the proterozoic hormuz evaporites, southern Iran. M.Sc. Thesis. University of Oregon, Wiley, New York, pp. 57–64.

Hurtgen, M.T., Arthur, M.A., Suits, N.S., Kaufman, A.J., 2002. The sulfur isotopic composition of Neoproterozoic seawater sulfate: implications for a snowball earth? Earth Plant. Sci. Lett. 203, 413–429.

Husseini, M.I., Husseini, S.I., 1990. Origin of the Infracambrian salt basins of the Middle East. In: Brookes, J. (Ed.), Classic Petroleum Provinces, vol. 50. Geological Society Special Publication, pp. 279–292.

Jacobsen, S.B., Kaufman, A.J., 1999. The Sr, C and O isotopic evolution of Neoproterozoic seawater. Chem. Geol. 161, 37–57.

Kampschulte, A., Buhl, D., Strauss, H., 1998. The sulfur and strontium isotopic compositions of Permian evaporites from the Zechstein Basin, northern Germany. Geol. Rundschau 87, 192–199.

Kampschulte, A., Bruckschen, P., Strauss, H., 2001. The sulphur isotopic composition of trace sulphates in Carboniferous brachiopods: implications for coeval seawater, correlation with other geochemical cycles and isotope stratigraphy. Chem. Geol. 175, 165–189.

Kampschulte, A., Strauss, H., 2004. The sulphur isotopic evolution of Phanerozoic seawater based on the analysis of structurally substituted sulphate in carbonates. Chem. Geol. 204, 255–286.

Kaufman, A.J., Jacobsen, S.B., Knoll, A.H., 1993. The Vendian record of Sr and C isotopic variations in seawater: implications for tectonics and paleoclimate. Earth Plant. Sci. Lett. 120, 409–430.

Kaufman, A.J., Knoll, A.H., 1995. Neoproterozoic variations in the C-isotopic composition of seawater: stratigraphy and biogeochemical implications. Precamb. Res. 73, 27–49.

Kirkland, D.W., Evans, R., 1981. Source-rock potential of evaporitic environment. AAPG Bull. 65, 181–190.

Kumar, V., 1999. Eocambrian sedimentation in Nagaur-Ganganagar evaporite Basin, Rajasthan. J. Indian Assoc. Sedimentol. 18, 201–210.

Mazumdar, A., Bhattacharya, S.K., 2004. Stable isotopic study from late Neoproterozoic–early Cambrian (?) sediments from Nagaur-Ganganagar Basin, western India: possible signatures of global and regional C-isotopic events. Geochem. J. 38, 163–175.

McKerrow, W.S., Scolese, C.R., Brasier, M.D., 1992. Early Cambrian continental reconstruction. J. Geol. Soc. Lond. 149, 599–606.

Meert, J.G., Lieberman, B.S., 2004. A palaeomagnetic and palaeobiogeographic perspective on latest Neoproterozoic and early Cambrian tectonic events. J. Geol. Soc. Lond. 16, 1–11.

Megonigal, J.P., Hines, M.E., Visscher, P.T., 2003. Anaerobic metabolism: linkages to trace gases and aerobic processes. In: Holland, H.D., Turekian, K.K. (Eds.), Treatise on Geochemistry, Biogeochemistry, vol. 8. Elsevier Pergamon, pp. 317–424.

Melezhik, V.A., Gorokhov, I.M., Fallick, A.E., Gjelle, S., 2001. Strontium and carbon isotope geochemistry applied to dating of carbonate sedimentation: an example from high-grade rocks of the Norwegian Caledonides. Precamb. Res. 108, 267–292.

Milliken, K.L., 1979. The silicified evaporite syndrome—two aspects of silicification history of former evaporite nodules from southern Kentucky and northern Tennessee. J. Sed. Petrol. 49, 245–256.

Mishra, A., 1998. Mineralogy and petrography of the Hanseran Evaporite Group of Rocks, Bore Hole no. P-4, Near Lakhasar, Bikaner District, Rajasthan. Unpublished M.Phil. Thesis. University of Delhi, 44 pp.

Misi, A., Veizer, J., 1998. Neoproterozoic carbonate sequences of the Una Group, Ireci Basin, Brazil: chemostratigraphy, age and correlation. Precamb. Res. 89, 87–100.

Montanez, I., Osleger, D.A., Baneer, J.L., Mack, L.E., Musgrove, M., 2000. Evolution of the Sr and C isotope composition of Cambrian Oceans. GSA Today 10, 1–7.

Nicholas, C.J., 1996. The Sr isotopic evolution of the oceans during the 'Cambrian explosion'. J. Geol. Soc. Lond. 153, 243–254.

Palmer, M., Edmond, J.M., 1989. The strontium isotope budget of the modern ocean. Earth Plant. Sci. Lett. 92, 11–26.

Pandit, M.K., Sial, A.N., Jamrani, S.S., Ferreira, V.P., 2001. Carbon isotopic profile across the Bilara Group rocks of Trans-Aravalli Marwar Supergroup in western India: implications for Neoproterozoic–Cambrian transition. Gondwana Res. 4, 387–394.

Pareek, H.S., 1981. Basin configuration and sedimentary stratigraphy of western Rajasthan. J. Geol. Soc. India 22, 517–527.

Peryt, T.M., Halas, S., Kovalevych, V.M., Petrychenko, O.Y., Dzhiorididze, N.M., 2005. The sulphur and oxygen isotopic composition of lower Cambrian anhydrites in east Siberia. Geological Quarterly 49, 235–242.

Peters, K.E., Clark, M.E., Das Gupta, U., McCaffrey, Lee, C.Y., 1995. Recognition of an infracambrian source rock based on biomarkers in the Baghewala-1 oil, India. AAPG Bull. 79, 1481–1494.

Rathore, S.S., Venkateshan, T.R., Srivastava, R.K., 1999. Rb–Sr isotopic dating of Neoproterozoic (Malani Group) magmatism from south west Rajasthan, India: evidence of a younger Pan-African thermal event by Ar–Ar studies. Gondwana Res. 2, 246–271.

Reinick, H.E, Singh, I.B., 1980. Depositional Sedimentary Environments. Springer-Verlag, Berlin.

Schröder, S., Scheiber, B.C., Amthor, J.E., Matter, A., 2004. Stratigraphy and environmental conditions of the terminal Neoproterozoic–Cambrian period in Oman: evidence from sulphur isotopes. J. Geol. Soc. Lond. 161, 489–499.

Shen, Y., Schidlowski, M., Chu, X., 2000. Biogeochemical approach to understanding phosphogenic events of the terminal Proterozoic to Cambrian. Palaeogeogr. Palaeoclimatol. Palaeoecol. 158, 99–108.

Shields, G., Kimura, H., Yang, J., Gammon, P., 2004. Sulphur isotopic evolution of Neoproterozoic–Cambrian seawater: new francolite-bound sulphate δ34S. Chem. Geol. 204, 163–182.

Shields, G.A., Strauss, H., Howe, S.S., Siegmund, H., 1999. Sulphur isotope composition of sedimentary phosphorites from the basal Cambrian of China: implications for Neoproterozoic–Cambrian biogeochemical cycling. J. Geol. Soc. Lond. 156, 943–955.

Siedlecka, A., 1972. Length-slow chacydony and relicts of sulphates—evidence of evaporitic environments in the Upper Carboniferous and Permian red beds of Bear Island, Svalbard. J. Sed. Petrol. 42, 812–816.

Staudt, W., Scoonen, M.A.A., 1995. Sulfate incorporation into sedimentary carbonates. In: Vairavamurthy, M.A., Schoonen, M.A.A. (Eds.), Geochemical Transformation of Sedimentary Sulfur. American Chemical Society, pp. 332–345.

Strauss, H., 1997. The isotopic composition of sedimentary sulfur through time. Palaeogeogr. Palaeoclimatol. Palaeoecol. 132, 7–118.

Strauss, H., 2004. 4 Ga of seawater evolution: evidence from the sulphur isotopic composition of sulphate. In: Amend, J.P., Edwards, K.J., Lyons, T.W. (Eds.), Sulphur Biogeochemistry—Past and Present. GSA, Special Paper 379. Boulder, pp. 195–205.

Strauss, H., Banerjee, D.M., Kumar, V., 2001. The sulfur isotopic composition of Neoproterozoic to early Cambrian seawater-evidence from the cyclic Hanseran evaporates, NW India. Chem. Geol. 175, 17–28.

Tennant, C.B., Berger, R.W., 1957. X-ray determination of dolomite–calcite ratio of carbonate rock. Am. Miner. 42, 23–29.

Veizer, J., Ala, D., Azmy, K., Bruckschen, P., Buhl, D., Bruhn, F., Carden, G.A.F., Diener, A., Ebneth, S., Godderis, Y., Jasper, T., Korte, C., Pawallek, F., Podlaha, O.G., Strauss, H., 1999. 87Sr/86Sr δ13C and δ18O evolution of Phanerozoic seawater. Chem. Geol. 161, 59–88.

Vinogradov, V.I., Pokrovskiy, B.G., Pustylnikov, A.M., Muravyev, V.I., Shatsiy, G.V., Buyakayte, M.I., Lukanin, A.O., 1994. Isotopnogeochimicheskie osobennosti I vozrast verkhenodokembriyskikh otlozheniy zapada Sibirskoy platoformy. Litol. Polezn. Iskop. 4, 49–76.

Walter, M.R., Veevers, J.J., Calver, C.R., Gorjan, P., Hill, A.C., 2000. Dating the 840–544 Ma Neoproterozoic interval by isotopes of strontium, carbon, and sulfur in seawater, and some interpretative models. Precamb. Res. 100, 371–433.